

Some Aerodynamic Performances of Small Size Compressor and Turbine Stages

I.V. Gaydamaka¹, A.V. Efimov², M.Ja. Ivanov¹,
O.I. Ivanov², R.Z. Nigmatullin¹, N.I. Ogarko²

¹ The Turbine Department

² The Compressor Department

Central Institute of Aviation Motors (CIAM)
2, Aviamotornaya St., Moscow, 111116, Russia
Phone: +007-095-362-1386, Fax: +007-095-362-1386
E-mail: ivanov@ciam.ru

KEYWORDS: MEMS, microcompressors,
microturbine, aerodynamics.

**SMALL SIZE CENTRIFUGAL
COMPRESSOR**

ABSTRACT

Aerodynamic performances of small one stage radial compressor and turbine with rotor sizes near 40 mm are investigated. These components may be considered as the prototype of energetic microturbine components. Main attention is paid of possible efficiency increasing for such type radial compressor and turbine. Typical local and integral parameters of compressor and turbine stages are demonstrated.

INTRODUCTION

During last decade some leader gas turbine centers begun intensive development of microturbine as real alternative of compact sources of electrical and thermal energy. Such type results and wide references for microturbine can be found in Epstein (1997, 2000): Ultra-Micro GT (2001), Power MEMS (2002). The complex problem for microturbine development is high efficiency of main components – compressor and turbine.

This paper considers aerodynamics of small one stage radial compressor and turbine. Study of flow picture and main parameters in compressor and turbine stages is fulfilled with help of CFD methodology.

The first part of paper presents the results of aerodynamic design and performance study for the centrifugal compressors with pressure ratio $\pi_c^* = 3.0$ and 4.0. The second part presents the same results for the radial microturbine.

Centrifugal compressor on $\pi_c^* = 3.0$

The centrifugal compressor was designed for the following initial data:

Corrected air flow rate -	$G_{a\text{ cor}} = 13 \text{ g/s}$;
Total pressure ratio -	$\pi_c^* = 3.0$;
Impeller outer diameter -	$D_2 = 40 \text{ mm}$;
Inlet air temperature -	$T_1^* = 288 \text{ K}^\circ$;
Inlet air pressure -	$P_1^* = 101.3 \text{ kPa}$;
Corrected rotational speed	$n_{\text{cor}} = 210000 \text{ rpm}$.

The compressor consists from two blade rows: rotating impeller and radial diffuser.

The choice of main geometrical parameters was carried out using the design experience concerning real centrifugal compressors of high efficiency.

Determinant design data for the centrifugal impeller are: inlet β_{1b} and outlet β_{2b} blade angles (angle between tangent to mean line of the profile and tangential direction), number of blades Z , relative width of the channel b/D_2 , diameter relation D_1/D_2 and variation of the channel section area along length.

Due to absence of manufacturing and technological experience of micro compressors, the centrifugal impeller was designed without an axial part. Design of usual centrifugal impellers with radial cascade shows that because of flow turn from axial direction to radial one the flow at the blade inlet is non-uniform. Flow velocity C_1 and, consequently, flow angles β_1 at tip surface increase and at hub surface decrease. To reduce the negative influence of non-uniformity of flow, inlet relative Mach number was taken $M_{w1} \sim 0.5 \dots 0.55$.

Inlet flow passage dimensions for the centrifugal impeller are chosen from a condition to keep inlet relative flow angle at the blades of the order $\beta_1 = 30^\circ$.

As result of a number of preliminary considerations a diameter of inlet section for the centrifugal impeller $D_1 = 14$ mm and width of blades at inlet $b_1 = 3$ mm were chosen. Thus $D_1/D_2 = 0.35$ and $b_1/D_2 = 0.075$. Average flow velocity in absolute motion at inlet section of rotor blades is $C_1 = 91.9$ m/s and Laval number $\lambda_1 = 0.296$ ($M_1 = 0.272$). Flow angle in relative motion at rotor blades is $\beta_1 = 30.85^\circ$, relative flow velocity is $W_1 = 179.3$ m/s and Laval number $\lambda_{w1} = 0.566$ ($M_{w1} = 0.53$)

To reduce expansion of channels and to decrease a degree of aerodynamic deceleration, the centrifugal impeller is executed with variable width, decreasing to the outlet. The channel width decreases from 3 mm at inlet and up to 1 mm at outlet. The accepted number of blades of the impeller: $Z = 8$.

Initial data for blading design for the centrifugal impeller are geometrical angles of mean line of the blade profile at inlet $\beta_{1b} = 35^\circ$ and at outlet $\beta_{2b} = 76^\circ$. Blades have constant profile along height except for a zone, close to disk, where the thickness of the profile is increased due to rounding (smoothing). Maximum thickness of blades is 2 mm.

Vaneless diffuser of the compressor is characterized by relative size $D_3/D_2 = 1.125$ and has constant channel width $b_3 = b_2 = 1.0$ mm. Radial diffuser has the relative value $D_4/D_3 = 1.33$ and constant channel width $b_4 = b_3 = 1.0$ mm. Thus the radial diffuser has the degree of expansion $F_4/F_3 = 2.4$.

The design of radial diffuser was performed similarly. Geometrical angle of the blade profiles mean line at inlet is $\alpha_{3b} = 12^\circ$ and at outlet is $\alpha_{4b} = 24^\circ$. Number of diffuser blades $Z = 10$. Maximum thickness of blades is 1 mm.

Preliminary average parameter calculations of the centrifugal compressor has shown, that at the total pressure ratio π^* up to 3.0 and air mass flow rate $G_{a\text{cor}} = 13$ g/s it is possible to expect adiabatic efficiency values $\eta^*_{ad} = 0.6$.

The 3D Navier-Stokes calculations of viscous flow in the flow passage of the centrifugal compressor were fulfilled. Calculations were performed for zero tip clearance value (and without disc friction losses). These calculations allow as to study the flow structure in the compressor flow passage as to obtain integral parameters of the compressor.

Mach number contours in different sections of flow passage are shown in Fig. 1-3. From the figures it is clear, that there are areas of diffuser character of flow in the centrifugal impeller channels, which can lead to formation of flow separation. There is a large separation zone at the pressure side of radial diffuser.

Some integral parameters of the centrifugal compressor for the several air flow rates at design rotational speed are presented in Table 1.

Table 1

G	π^*_c	Efficiency
13.5	3.15	0.69
14.4	3.06	0.68
15.2	2.84	0.647
15.5	2.715	0.618

The results of the calculations allow to expect that it is possible to achieve adiabatic efficiency $\eta^*_{ad} = 0.6 \dots 0.65$ in micro compressor at pressure ratio $\pi^* = 3.0$ and air flow rate $G_{a\text{cor}} = 15$ g/s.

Centrifugal compressor on $\pi^*_c = 4.0$

Geometrical parameters of centrifugal impeller for the case $\pi^*_c = 4.0$ were taken the same as for the version with $\pi^*_c = 3.0$. The increase of π^*_c from 3.0 to 4.0 is achieved by the increase of rotor rotational speed from $n_{\text{cor}} = 210000$ rpm to 250000 rpm.

The radial extent of vaneless diffuser is characterized by the ratio $D_3/D_2 = 1.125$ and is equal to $\Delta R = 2.5$ mm. The diffuser has $D_4/D_3 = 1.33$ and degree of expansion $F_4/F_3 = 2.4$.

Flow angle in absolute motion at the radial diffuser inlet is $\alpha_3 = 10.4^\circ$, and Laval number is $\lambda_3 = 0.851$ ($M_3 = 0.829$). In comparison with the compressor on $\pi^*_c = 3.0$ the flow angle α_3 decreases by 1.5° , and Laval number increases by 6%.

The average parameter calculation results of the compressor on $\pi^*_c = 4.0$ and the accepted geometry flow path, which practically coincides with the geometry of the compressor on $\pi^*_c = 3.0$, allows at the first stages to limit the investigations by the compressor on $\pi^*_c = 3.0$.

To achieve the total pressure ratio $\pi^*_c = 4.0$ and air flow rate $G_{a\text{cor}} = 15$ g/s it is sufficient to increase the rotational speed from $n_{\text{cor}} = 210000$ rpm to $n_{\text{cor}} = 250000$ rpm, i.e. by 19 %. Using the obtained result one can then, if necessary, correct the design of the centrifugal compressor on $\pi^*_c = 4.0$

RADIAL MICROTURBINE

In the designed model micro gas turbine engine the pressure ratio at the designed point has been chosen equal to 3.0. As the rotor of the model turbine is supposed to be produced from traditional materials but not from single crystal Si or SiC, the turbine inlet temperature is chosen 950°C (1223 K). The rotational speed $n = 210000$ rpm corresponds to tip circumferential speed ~ 440 m/sec (the rotor diameter is 40 mm).

The compressor inlet total pressure losses are taken about 1,5% and the combustor losses – 10%. Thus, if the atmospheric pressure $p_a = 101.3$ kPa then the turbine inlet total pressure $p_0^* = 269.4$ kPa. The design value of compressor inlet air mass flow rate is 13.1 g/s. Taking into account the fuel mass flow

(standard hydrocarbon fuel is supposed to be used) the inlet turbine gas mass flow rate is $G_0 = 13.4$ g/s.

The geometrical parameters of the microturbine rotor $D_2 = 24$ mm and $h_2 = 2$ mm have been chosen.

A characteristic feature of the radial microturbine is 2D vane and blade configurations, i.e. all the blades have the same profile form along the span. Therewith the flowpath height has not been changed from the inlet towards the outlet. These limitations are imposed by micromachine manufacturing process. The flowpath geometric shape and the blades forms are well shown in Fig. 10.

Similar to Epstein (2000), the microturbine rotor edge thickness may be equal to 25 microns. In the model turbine the edge thickness has been chosen 0.25 mm. As the nozzle vanes do not have the centrifugal force load then the trailing edges thickness is 0.15 mm.

The outlet rotor static pressure was accepted to the atmospheric one $p_2 = 101.3$ kPa, as this configuration of the exhaust system cannot be considered as an efficient diffuser. The outlet flow angle in absolute motion has been chosen 90° (the angle counting is from the circumferential direction).

For the traditional centripetal turbines with radial leading edge direction the optimal blade-jet speed ratio value $u_1/C_{is} = 0.7$. As for the designed turbine the value of this parameter is less so rotor inlet angle in relative motion is less than 90° . It requires the use non-radial leading edges. The axial exit flow direction is provided by the corresponding reaction degree choice.

The table 2 shows the preliminary gas dynamic analysis results without calculation of the rotor blades tip clearance losses and disk friction losses (in the calculation the Navier-Stokes losses were used).

Table 2

Parameter	Dimension	Value
α_0	deg	90
u_1	m/s	439.8
α_1	deg	11.88
c_1	m/s	488.8
β_1	deg	69.1
w_1	m/s	107.8
u_2	m/s	263.9
α_2	deg	90.6
c_2	m/s	256.8
β_2	deg	44.5
w_2	m/s	366.3
u_1/C_{is}	-	0.591
ρ	-	0.5
η_{tt}	-	0.756
η_{ts}	-	0.68

0 – turbine inlet; 1- rotor inlet; 2- rotor outlet.

The radial microturbine nozzle vane and rotor blade profiling was carried out by conformal transformation of the aerodynamically perfect straight cascade profiles. Also the 3D viscous flow calculations in the turbine flowpath were carried out.

Two nozzle and two rotor variants were designed. The original nozzle variant (Nozzle 1) has the satisfactory velocity distribution except the outlet part of suction surface where small local separation is observed (Fig. 4). This surface area redesign for Nozzle 2 allowed to avoid this local separation (Fig. 7) and to increase the nozzle efficiency. According to calculation results the total loss coefficient has been decreased by 10%. Fig.5 shows Laval number λ (ratio of isentropic flow velocity to critical velocity) distribution along the Nozzle 1 vane boundary surface.

The characteristic feature for the Rotor 1 is the presence of the intensive separation at the suction surface outlet area (Fig.4). The static pressure in this area has slight positive gradient. Fig. 6 shows isentropic Laval number distribution along the airfoil surface. The laminar flow regime due to low Re number leads to the boundary layer separation practically at the beginning of the decelerating part.

To remove this separation the number of blades for Rotor 2 was increased to $Z=22$ (for Rotor 1 $Z=17$). Besides the trailing edge taper was decreased and outlet profile section geometry was changed to reversed curvature. It allowed removing the flow separation at the blade suction surface (Fig.7). However in spite of practically constant static pressure value in the outlet part of suction surface (Fig.8) the boundary layer thickness anyway is increased. The nozzle and rotor redesign of the above mentioned turbine leads to noticeable positive effect. For example, the turbine total-to-total efficiency rises from $\eta_{tt(1)} = 0.758$ to $\eta_{tt(2)} = 0.789$, and total-to-static efficiency from $\eta_{ts(1)} = 0.683$ to $\eta_{ts(2)} = 0.710$. As for 1D analysis, the influences of the rotor blades tip clearance and disc friction losses were not taken into account.

Fig.9 shows Mach number distribution in the middle of the blade-to-blade channels in the projection to the meridional plane and Fig.10 presents the corresponding meridional velocity components vectors. The velocity distributions in absolute motion in the nozzle vane as well as in the rotor and at the turbine exit in relative motion are presented in it. The flow on the rotor disk separates near the rotor trailing edges with extensive circulation flow.

The fulfilled analysis has shown that despite the small dimensions of micro turbines it may have relatively high efficiency and there are some possibilities for its further rise.

ACKNOWLEDGEMENTS

This research was sponsored by NEDO International Joint Research Project (J13-30). The authors wish to express their gratitude to Professor T.Nagashima of the University of Tokyo for the fruitful discussions and problem formulation.

REFERENCES

Epstein A.H. et al., 1997, "Micro-heat engines, gas turbines and rocket engines". The MIT Microengine Project, AIAA Paper N 97-1773.

Epstein A.H. et al., 2000, "Shirtbutton-sized gas turbines: the engineering challenges of micro high speed rotating machinery." 5.0 Overview technical paper. 10 p.

Ultra-Micro GT, 2001, J. of the Gas Turbine Society of Japan, Vol. 29, No. 4.

Power MEMS 2002. International Workshop on Power MEMS. Extended Abstracts. Tsukuba, Japan, Nov. 12-13, 2002.

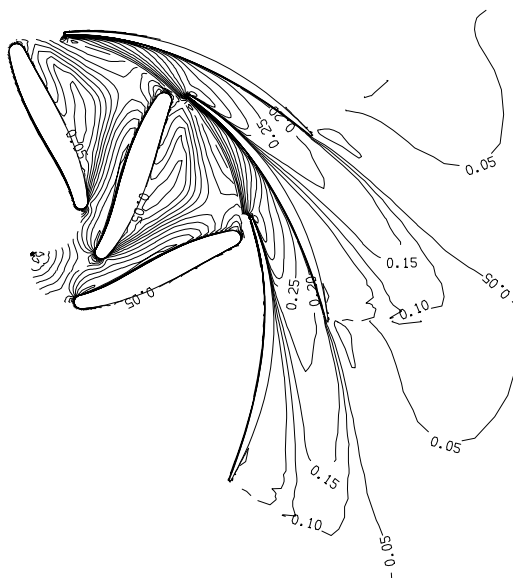


Fig.1. Mach number contours close to hub section.

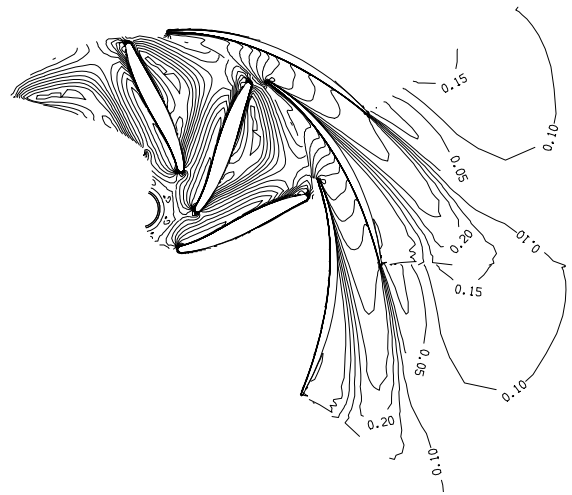


Fig.2. Mach number contours at mean section.



Fig.3. Mach number contours in mean meridional section.

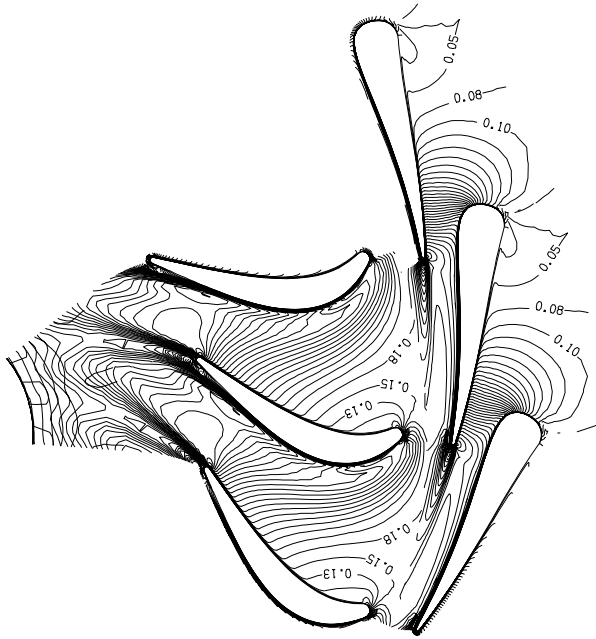


Fig.4. Mach number contours at mean section of flow passage (Version: Nozzle1+Rotor1).

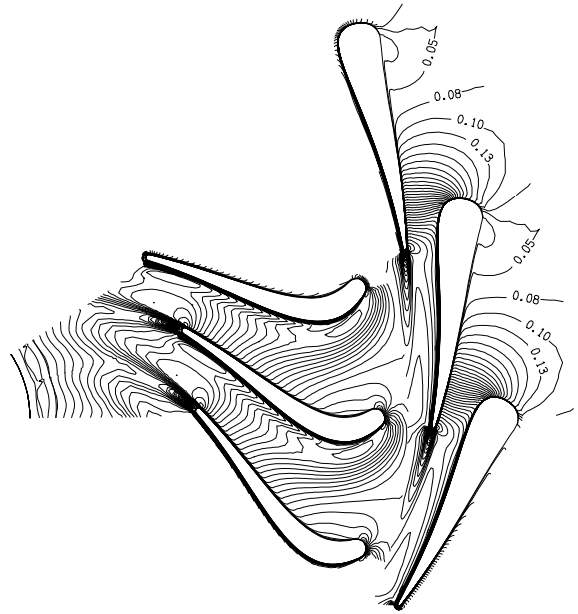


Fig.7. Mach number contours at mean section of flow passage (Version: Nozzle2+Rotor2).

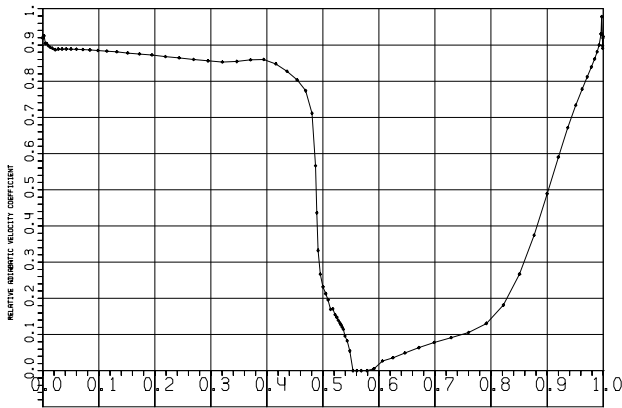


Fig.5. Isentropic Laval number distribution along the profile arc length of Nozzle1 (mean section)

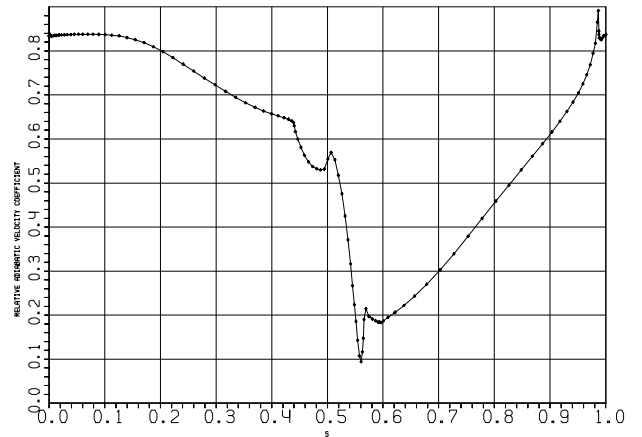


Fig.8. Isentropic Laval number distribution along the profile arc length of Rotor2 (mean section)

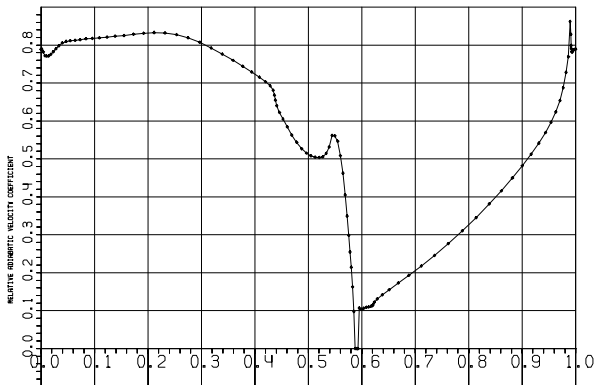


Fig.6. Isentropic Laval number distribution along the profile arc length of Rotor1 (mean section)

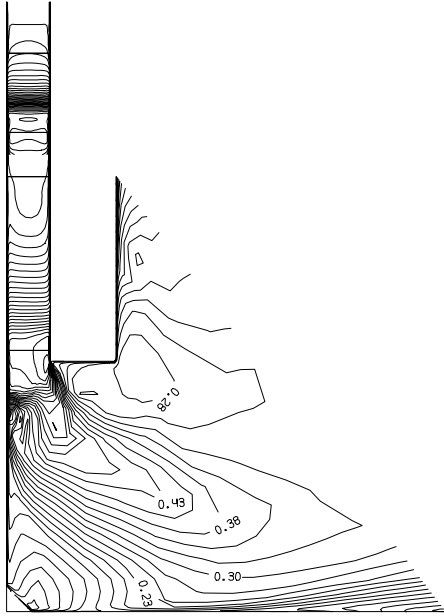


Fig.9. Mach number contours in mean blade-to-blade section.

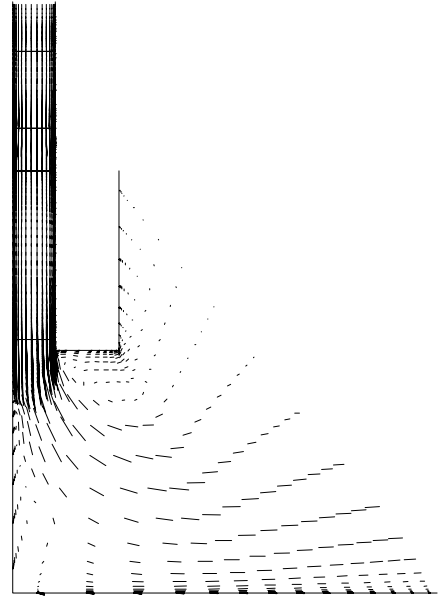


Fig.10. Velocity vector field in mean blade-to-blade section.